Geophysical Journal International

Geophys. J. Int. (2016) **206,** 1487–1491
Advance Access publication 2016 June 27
GJI Seismology

doi: 10.1093/gji/ggw239

EXPRESS LETTER

Seismological investigation of the 2016 January 6 North Korean underground nuclear test

Lian-Feng Zhao,[1] Xiao-Bi Xie,[2] Wei-Min Wang,[3] Jin-Lai Hao[1] and Zhen-Xing Yao[1]

[1]*Key Laboratory of Earth and Planetary Physics, Institute of Geology and Geophysics, Chinese Academy of Sciences, Beijing* 100029, *China.*
E-mail: zhaolf@mail.iggcas.ac.cn
[2]*Institute of Geophysics and Planetary Physics, University of California at Santa Cruz, Santa Cruz, CA* 95064, *USA*
[3]*Key Laboratory of Continental Collision and Plateau Uplift, Institute of Tibetan Plateau Research, Chinese Academy of Sciences, Beijing* 100101, *China*

Accepted 2016 June 22. Received 2016 June 21; in original form 2016 January 25

SUMMARY

Seismology plays an important role in characterizing potential underground nuclear tests. Using broad-band digital seismic data from Northeast China, South Korea and Japan, we investigated the properties of the recent seismic event occurred in North Korea on 2016 January 6. Using a relative location method and choosing the previous 2006 explosion as the master event, the 2016 event was located within the North Korean nuclear test site, with its epicentre at latitude 41.3003°N and longitude 129.0678°E, approximately 900 m north and 500 m west of the previous event on 2013 February 12. Based on the error ellipse, the relocation uncertainty was approximately 70 m. Using the *P*/*S* spectral ratios, including Pg/Lg, Pn/Lg and Pn/Sn, as the discriminants, we identify the 2016 event as an explosion rather than an earthquake. The body-wave magnitude calculated from regional wave Lg is m_b(Lg) equal to 4.7 ± 0.2. Adopting an empirical magnitude–yield relation, and assuming that the explosion is fully coupled and detonated at a normally scaled depth, we find that the seismic yield is about 4 kt, with the uncertainties allowing a range from 2 to 8 kt.

Key words: Seismic monitoring and test-ban treaty verification; Computational seismology; Wave propagation.

1 INTRODUCTION

According to the international media and nuclear monitoring agencies, a seismic event with a magnitude ~5.0 occurred near the North Korean nuclear test site (NKTS) at 01:30 (UTC) on 2016 January 6. Earlier, nuclear tests had been conducted at NKTS on 2006 October 9, 2009 May 25 and 2013 February 12. Regional seismic phases from these nuclear tests were recorded by broad-band digital stations installed in Northeast China, South Korea and Japan. Fig. 1 shows examples of broad-band waveforms from these nuclear tests and the 2016 event, recorded at station MDJ. All four seismograms show highly consistent waveforms, abrupt primary *P*-wave arrivals, weak Lg phases and well-developed short-period Rayleigh waves, all typical for shallow explosive sources (e.g. Richards & Kim 2007).

The three major tasks for seismological investigations of potential nuclear tests are: (i) finding the epicentre of the event (Schaff & Richards 2004; Schlittenhardt *et al*. 2010; Selby 2010; Wen & Long 2010; Murphy *et al*. 2013; Zhang & Wen 2013; Zhao *et al*. 2014), (ii) identifying the characteristics of the event to determine if it is an explosion or an earthquake (e.g. Richards & Kim 2007; Zhao *et al*. 2008; Shin *et al*. 2010; Murphy *et al*. 2013); and (iii) determining the seismic magnitude and estimating the seismic yield (e.g. Zhao *et al*. 2008, 2012, 2014; Murphy *et al*. 2013; Zhang & Wen 2013). The 2016 event generated abundant regional seismic signals over distances from a few hundred to a few thousand kilometres. We collected broad-band digital waveforms recorded on the China National Digital Seismic Network (CNDSN), the Global Seismic Network (GSN) and the Japan F-NET to investigate this event. The results confirm that this is another underground nuclear test. In the remainder of this paper, we report the details of our investigations. For convenience, we refer to the events in 2006, 2009, 2013 and 2016 as NKT1, 2, 3 and 4, respectively.

2 HIGH-PRECISION EVENT RELOCATION

Relying on Pn differential traveltimes and the selection of a master event, the relative location method (Schaff & Richards 2004; Selby 2010; Wen & Long 2010; Murphy *et al*. 2013; Zhang & Wen 2013; Zhao *et al*. 2014) provides highly accurate event locations relative to the master event. Zhao *et al*. (2014) used this method to determine the origin times and locations of NKT2 and NKT3 relative to NKT1. The Pn differential traveltimes from NKT4 provide us with information to determine the origin time and location of this event and to

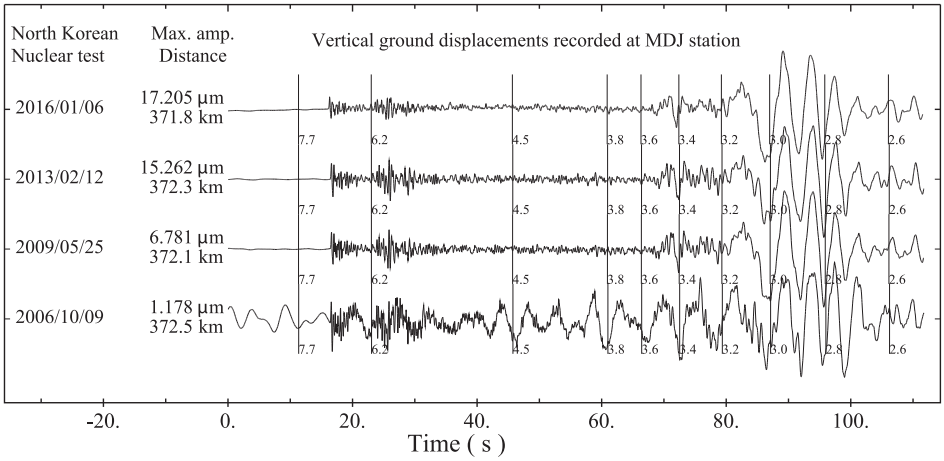

Figure 1. Normalized vertical-component displacement seismograms recorded at MDJ for three North Korean nuclear tests in 2013, 2009 and 2006, along with the waveforms from the recent event in 2016. The event dates, maximum amplitudes and epicentre distances are listed on the left. Marks on the waveforms indicate apparent group velocities. These waveforms are highly consistent and characterized by clear impulsive *P*-wave onset, relatively weak Lg phases and 3- to 5-s period Rayleigh waves.

update the locations of NKT2 and NKT3 with improved accuracy. We still use NKT1 as the primary master event and adopt the origin time and location reported by the US Geological Survey (USGS) based on satellite images (Wen & Long 2010) to simultaneously constrain the locations and origin times for NKT2, NKT3 and NKT4. Seismograms from 95 regional seismic stations are used in the relocation (Supporting Information Fig. S1, Tables S1 and S2). To calculate the differential traveltimes (Schaff & Richards 2004), the Pn waveforms are bandpass filtered between 2.0 and 10.0 Hz and sampled in a 2-s time window starting from the Pn first arrival (Supporting Information Fig. S2). Then, cross-correlations are calculated between waveforms from different events recorded at the same stations to obtain 238 Pn differential traveltimes (Supporting Information Table S2).

Previous North Korean nuclear tests were detonated close to each other. For a given station, the instrument and site responses are the same, and propagation paths to different events are nearly the same, except for the short section beneath the NKTS. The differential traveltimes between the different events mainly resulted from their origin times, epicentre locations, burial depths and the Pn velocity beneath the test site. Because of the trade-off between depth and origin time, we include only the origin times in the calculation. Finally, a model with 10 parameters is created: the longitudes and latitudes of NKT2, NKT3 and NKT4; the Pn velocity beneath the test site; and the three origin times, which are used to fit the observed Pn differential traveltimes. Because the stations are unevenly distributed azimuthally, we group the differential traveltimes into 20° azimuthal bins and set up a weighting function to balance their contributions. All results, along with their uncertainties, are listed in Table 1. The best-fit epicentre of NKT4 is [41.3003°N, 129.0678°E]. Based on the error ellipses (Allan 1972), the uncertainty of the relative location is approximately 70 m. In Fig. 2, the epicentre of NKT4 is approximately 900 m north and 500 m west of NKT3, and 3700 m and 1000 m away from NKT1 and NKT2, respectively. NKT4 appears to be on the same mountain as NKT2 and NKT3 but on a different side. The best-fit origin time for NKT4 is 01:30:00.9706 ± 0.0015 UTC. The uppermost mantle *P*-wave velocity beneath the test site is estimated to be 7.99 ± 0.11 km s^{-1}, which is consistent with previous studies (e.g. Wang *et al*. 2003; Hearn *et al*. 2004; Liang *et al*. 2004; Zhao *et al*. 2012, 2014). All parameters obtained are relative and by assuming that the parameters for NKT1 are accurate.

3 EVENT DISCRIMINATION BASED ON *P*/*S*-TYPE SPECTRAL RATIOS

Ideally, an isotropic explosion source mainly generates *P* waves and is a poor *S*-wave source. In contrast, a natural earthquake is caused by fault slips, which can be described by a double-couple source that radiates abundant *S* waves. Therefore, the *P*- and *S*-wave energy radiated from a seismic source can be an important indicator for discriminating the properties of the source. Traditionally, the differences between body-wave magnitude and surface wave magnitude were used to discriminate explosion sources from earthquake sources at global distances. Similarly, the *P*/*S*-type spectral ratios of regional phases, that is, Pg/Lg, Pn/Lg and Pn/Sn, have been widely used for the same purpose at regional distances (Taylor *et al*. 1989; Walter *et al*. 1995; Xie 2002; Fisk 2006; Richards & Kim 2007). Because of the randomness caused by certain local effects, observations from individual stations may encounter

Table 1. Best-fit locations and origin times of the North Korean nuclear tests.

NK nuclear test	Data (yyyy/mm/dd)	Origin time (hh/mm/ss)	Standard deviation (s)	Latitude (°N)	Longitude (°E)	Location uncertainty (m)
NKT1	2006/10/09	01:35:28.0000[a]	0	41.2874[b]	129.1083[b]	0
NKT2	2009/05/25	00:54:43.1142	0.0023	41.2940	129.0775	
NKT3	2013/02/12	02:57:51.2741	0.0015	41.2918	129.0733	
NKT4	2016/01/06	01:30:00.9706	0.0015	41.3003	129.0678	70

[a]From USGS.
[b]From satellite images (Wen & Long 2010; Zhao *et al*. 2014).

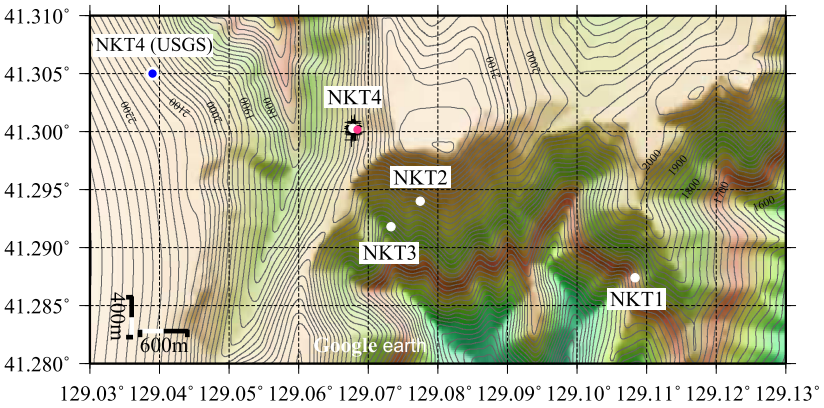

Figure 2. Topography and locations of the four NKTS events; white dots were obtained using all data, and the red dot for NKT4 was obtained using records from GSN and F-NET stations.

difficulty when separating explosions from earthquakes (e.g. Richards & Kim 2007), particularly at lower frequencies. This problem, however, can be overcome using network statistics (Zhao *et al*. 2008, 2014).

We use four NKTS explosions and four natural earthquakes near the NKTS to test the source discrimination (Supporting Information Table S3). The regional phases Pn, Pg, Sn and Lg are sampled from vertical-component displacement waveforms at stations with purely continental paths. After correcting for distance (Hartse *et al*. 1997; Zhao *et al*. 2008) and eliminating data with signal-to-noise ratios below 1.8, we calculate the *P*/*S* type spectral ratios Pg/Lg, Pn/Lg and Pn/Sn at individual stations. Fig. 3(a) shows examples of spectral ratios calculated for explosion NKT2 and an m_b 4.6 earthquake that occurred on 2002 April 16, and the different symbols represent observations from individual stations, with solid circles and error bars indicating network averaged mean values and their

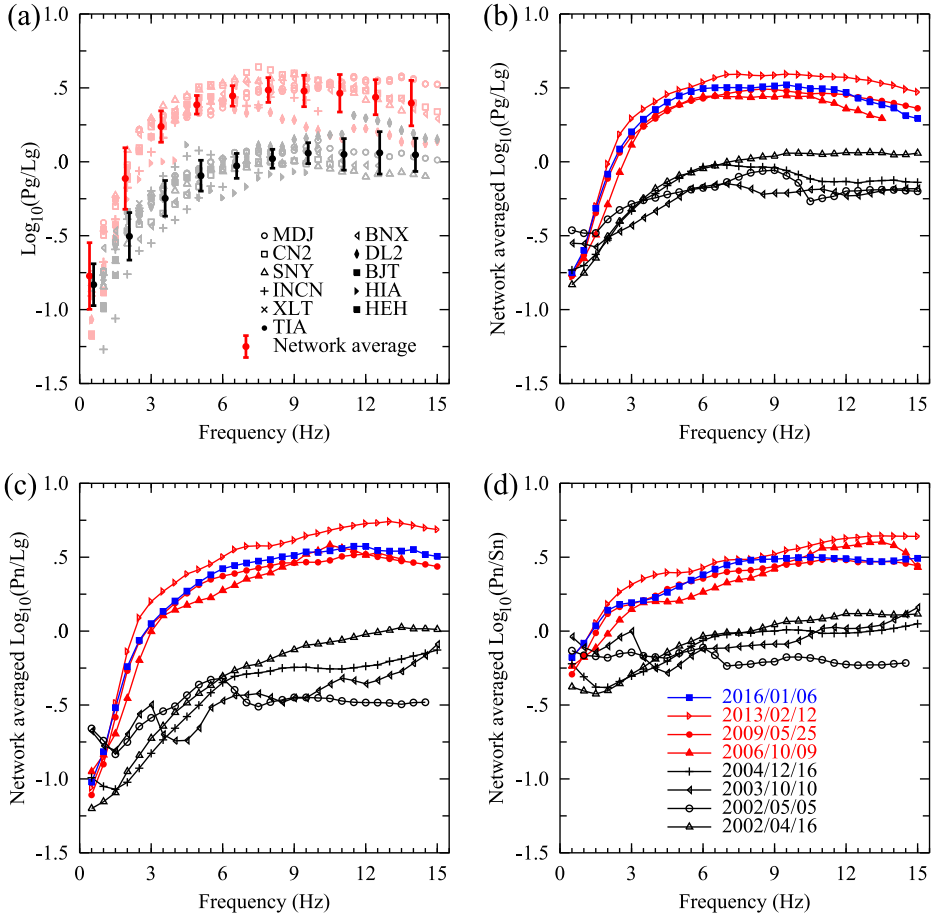

Figure 3. Spectral ratios for selected regional phases. (a) Comparisons of the Pg/Lg spectral ratios for NKT2 and an earthquake that occurred on 2002 April 16. Symbols indicate data from individual stations. Solid circles and error bars are network averages. Red and black colours indicate explosion and earthquake sources, respectively. (b–d) Pn/Lg, Pn/Sn and Pg/Lg spectral ratios from four NKTS events and four nearby earthquakes (the parameters are listed in Supporting Information Table S3).

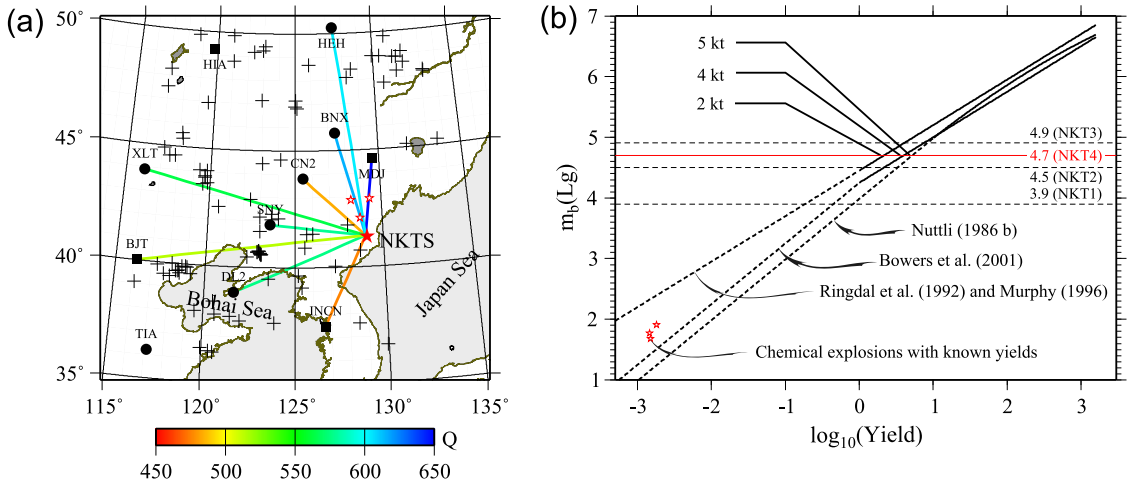

Figure 4. (a) Map showing the locations of the North Korean test site (solid red star) and the CNDSN (solid circles) and GSN (solid squares) stations used for the magnitude calculation and yield estimation. Also illustrated are the epicentres of the earthquakes (crosses) that occurred between December 1995 and January 2016 and three chemical explosions (open red stars) with known yields. (b) Empirical magnitude–yield relation; sections supported by observations are illustrated as solid lines and extrapolations are illustrated as dashed lines. The horizontal red line indicates the estimated magnitude, $m_b(\mathrm{Lg}) = 4.7$ for NKT4. Three chemical explosions with known yields (stars) are also illustrated.

standard deviations, and the red and black colours indicating explosions and earthquakes, respectively. These single-station observations show a clear tendency for explosive sources to radiate more *P*-wave energy relative to earthquakes. However, the single-station results are rather scattered, particularly at low and high frequencies. Conversely, the network average increases the reliability of the separation. Figs 3(b)–(d) show the network averaged spectral ratios from four NKTS explosions and four natural earthquakes, with the black symbols representing earthquakes, the red symbols indicating NKT1–3, and the blue symbols indicating NKT4. In all cases, the explosion and earthquake populations can be completely discriminated at frequencies above 2.0 Hz, thereby indicating that an underground nuclear explosion within this magnitude range that is detonated in the China–North Korea border region can be unambiguously screened by a regional seismic network.

4 EVENT MAGNITUDE AND YIELD ESTIMATION

The seismic yield of an underground nuclear explosion can be estimated through its magnitude using an empirical magnitude–yield relation (Nuttli 1986; Ringdal *et al*. 1992; Murphy 1996; Bowers *et al*. 2001; Zhao *et al*. 2008, 2012; Zhang & Wen 2013). We used an 11-station regional seismic network (Fig. 4a) to calculate the Lg-wave magnitude. The network and the Lg-wave magnitude were pre-calibrated with a historical data set composed of 99 regional events with both $m_b(P)$ and $m_b(\mathrm{Lg})$ measurements (Supporting Information Table S3), and a regional Lg-wave attenuation model (Zhao *et al*. 2008; Zhao *et al*. 2010). Using the calibrated network the Lg-wave magnitude for NKT4 is $m_b(\mathrm{Lg}) = 4.7 \pm 0.2$, which should be equivalent to global body-wave magnitude $m_b(P)$ and can be used with the empirical relations obtained based on the global body-wave magnitude (e.g. Nuttli 1986).

Because the NKTS is an uncalibrated test site, it is necessary to adopt a suitable empirical magnitude–yield relation from other calibrated region, for example, those at the Nevada test site (NTS; Nuttli 1986), Novaya Zemlya (Bowers *et al*. 2001) and East Kazakhstan (Ringdal *et al*. 1992; Murphy 1996; Fig. 4b). The North Korean test site is located in a stable platform. The tectonic sitting and upper-mantle Pn-wave velocity are similar to the test sits in platform areas, for example, East Kazakhstan or Novaya Zemlya, and unlike the NTS located in a more active region (Zhao *et al*. 2008, 2012, 2014; Murphy *et al*. 2013). Based on these, we choose the fully coupled hard-rock site equation by Bowers *et al*. (2001) for the NKTS. Using this relationship, the estimated yield for NKT4 is 4 kt. The ±0.2 magnitude measurement error, when transferred to yield, can cause an uncertainty between 2 and 8 kt. The above estimation assumes a normally scaled burial depth for the source. However, if the source is greatly overburied, the yield may be underestimated.

5 DISCUSSION AND CONCLUSIONS

Based on broad-band regional seismic data recorded in Northeast China, South Korea and Japan, we investigated the seismic characteristics of the 2016 January 6 event in North Korea and confirmed that the event was an underground nuclear test at the NKTS. Using a relative location method and NKT1 as the master event, the locations and origin times of NKT2, NKT3 and NKT4 were determined. In general, these results are consistent with that of previous reports (e.g. Wen & Long 2010; Zhang & Wen 2013; Zhao *et al*. 2014). Although the relative location method is rather accurate, certain errors may occur. The local 3-D structure near the source can cause additional scattering, which would complicate the waveforms and cause errors in the cross-correlations. For an example, the Pn waveform from the 2006 event presented certain differences with the records from other events because the location of the 2006 event was further east, and these differences may cause additional errors when locating the epicentre. The *P*/*S*-type spectral ratios are effective discriminants for separating explosions from earthquakes and are especially reliable if network statistics are used. By using the network average, the *P*/*S* spectral ratios can separate explosions from nearby earthquakes at frequencies above 2 Hz. This result indicates that if an underground nuclear test similar to the North Korean explosions is detonated in this region, then it will likely be discriminated by a regional seismic network. Since NKTS is an uncalibrated test site, and given the uncertainties in transferring empirical magnitude–yield relations to NKTS, replacing global m_b with $m_b(\mathrm{Lg})$, and allowing for differences in near source geology,

the yield estimate is uncertain between 2 and 8 kt which, furthermore, will still be greatly expanded when considering the source depth uncertainty.

ACKNOWLEDGEMENTS

We thank Prof T. Lay for discussions on this work. We would also like to thank the editors, Profs J. Renner and D. Agnew, and two anonymous reviewers for their constructive comments that greatly improved this manuscript. This research was supported by the National Natural Science Foundation of China (grants 41374065 and 41474036). The waveforms recorded at the CNDSN, GSN and F-NET stations used in this study were collected from the China Earthquake Network Center (CENC), the Data Management Centre of China National Seismic Network at the Institute of Geophysics, the China Earthquake Administration (SEISDMC, doi:10.11998/SeisDmc/SN; Zheng *et al*. 2010) at http://www.seisdmc.ac.cn (last accessed March 2016), the Incorporated Research Institutions for Seismology Data Management Center (IRIS DMC) at www.iris.edu (last accessed January 2016) and the National Research Institute for Earth Science and Disaster Prevention (NIED) at http://www.fnet.bosai.go.jp (last accessed January 2016). The source parameters for the three chemical explosions were provided by X.-K. Zhang at the Geophysical Exploration Center of China Earthquake Administration (GECCEA). Some figures were created using GMT (Wessel & Smith 1998).

REFERENCES

Allan, A.L., 1972. The error ellipse: a further note, *Surv. Rev.,* **21,** 387–390.

Bowers, D., Marshall, P.D. & Douglas, A., 2001. The level of deterrence provided by data from the SPITS seismometer array to possible violations of the Comprehensive Test Ban in the Novaya Zemlya region, *Geophys. J. Int.,* **146,** 425–438.

Fisk, M.D., 2006. Source spectral modeling of regional *P*/*S* discriminants at nuclear test sites in China and the former Soviet Union, *Bull. seism. Soc. Am.,* **96,** 2348–2367.

Hartse, H.E., Taylor, S.R., Phillips, W.S. & Randall, G.E., 1997. A preliminary study of regional seismic discrimination in central Asia with emphasis on western China, *Bull. seism. Soc. Am.,* **87,** 551–568.

Hearn, T.M., Wang, S.Y., Ni, J.F., Xu, Z.H., Yu, Y.X. & Zhang, X.D., 2004. Uppermost mantle velocities beneath China and surrounding regions, *J. geophys. Res.,* **109**, doi:10.1029/2003JB002874.

Liang, C.T., Song, X.D. & Huang, J.L., 2004. Tomographic inversion of Pn travel times in China, *J. geophys. Res.,* **109,** doi:10.1029/2003JB002789.

Murphy, J.R., 1996. Type of seismic events and their source descriptions, in *Monitoring a Comprehensive Test Ban Treaty*, eds Husebye, E.S. & Dainty, A.M., pp. 225–245, Kluwer.

Murphy, J.R., Stevens, J.L., Kohl, B.C. & Bennett, T.J., 2013. Advanced seismic analyses of the source characteristics of the 2006 and 2009 North Korean nuclear tests, *Bull. seism. Soc. Am.,* **103,** 1640–1661.

Nuttli, O.W., 1986. Yield estimates of Nevada test site explosions obtained from seismic Lg waves, *J. geophys. Res.,* **91,** 2137–2151.

Richards, P.G. & Kim, W.Y., 2007. Seismic signature, *Nat. Phys.,* **3,** 4–6.

Ringdal, F., Marshall, P.D. & Alewine, R.W., 1992. Seismic yield determination of Soviet underground nuclear explosions at the Shagan River test site, *Geophys. J. Int.,* **109,** 65–77.

Schaff, D.P. & Richards, P.G., 2004. Repeating seismic events in China, *Science,* **303,** 1176–1178.

Schlittenhardt, J., Canty, M. & Grunberg, I., 2010. Satellite earth observations support CTBT monitoring: a case study of the nuclear test in North Korea of Oct. 9, 2006 and comparison with seismic results, *Pure appl. Geophys.,* **167,** 601–618.

Selby, N.D., 2010. Relative locations of the October 2006 and May 2009 DPRK announced nuclear tests using international monitoring system seismometer arrays, *Bull. seism. Soc. Am.,* **100,** 1779–1784.

Shin, J.S., Sheen, D.H. & Kim, G., 2010. Regional observations of the second North Korean nuclear test on 2009 May 25, *Geophys. J. Int.,* **180,** 243–250.

Taylor, S.R., Denny, M.D., Vergino, E.S. & Glaser, R.E., 1989. Regional discrimination between NTS explosions and western United States earthquakes, *Bull. seism. Soc. Am.,* **79,** 1142–1176.

Walter, W.R., Mayeda, K.M. & Patton, H.J., 1995. Phase and spectral ratio discrimination between NTS earthquakes and explosions: 1. Empirical observations, *Bull. seism. Soc. Am.,* **85,** 1050–1067.

Wang, S.Y., Xu, Z.H. & Pei, S.P., 2003. Velocity structure of uppermost mantle beneath North China from Pn tomography and its implications, *Sci. China D,* **46,** 130–140.

Wen, L.X. & Long, H., 2010. High-precision location of North Korea's 2009 nuclear test, *Seismol. Res. Lett.,* **81,** 26–29.

Wessel, P. & Smith, W., 1998. New, improved version of the generic mapping tools released, *EOS, Trans. Am. geophys. Un.,* **79,** 579, doi:10.1029/98EO00426.

Xie, J., 2002. Source scaling of Pn and Lg spectra and their ratios from explosions in central Asia: implications for the identification of small seismic events at regional distances, *J. geophys. Res.,* **107,** doi:10.1029/2001JB000509.

Zhang, M. & Wen, L.X., 2013. High-precision location and yield of North Korea's 2013 nuclear test, *Geophys. Res. Lett.,* **40,** 2941–2946.

Zhao, L.F., Xie, X.B., Wang, W.M. & Yao, Z.X., 2008. Regional seismic characteristics of the 9 October 2006 North Korean nuclear test, *Bull. seism. Soc. Am.,* **98,** 2571–2589.

Zhao, L.F., Xie, X.B., Wang, W.M., Zhang, J.H. & Yao, Z.X., 2010. Seismic Lg-wave Q tomography in and around Northeast China, *J. geophys. Res.,* **115,** B08307, doi:10.1029/2009JB007157.

Zhao, L.F., Xie, X.B., Wang, W.M. & Yao, Z.X., 2012. Yield estimation of the 25 May 2009 North Korean nuclear explosion, *Bull. seism. Soc. Am.,* **102,** 467–478.

Zhao, L.F., Xie, X.B., Wang, W.M. & Yao, Z.X., 2014. The 12 February 2013 North Korean underground nuclear test, *Seismol. Res. Lett.,* **85,** 130–134.

Zheng, X.F., Yao, Z.X., Liang, J.H. & Zheng, J., 2010. The role played and opportunities provided by IGP DMC of China National Seismic Network in Wenchuan earthquake disaster relief and researches, *Bull. seism. Soc. Am.,* **100,** 2866–2872.

SUPPORTING INFORMATION

Additional Supporting Information may be found in the online version of this paper:

Figure S1. (a) Map showing the locations of the North Korean test site (red star) and the CNDSN (blue solid circles), GSN (black solid squares) and F-NET (triangles) stations used for the relocation. The inset map (b) displays the details of the station locations.

Figure S2. Pn waveform cross-correlations at selected stations between NKT4 (blue) and NKT3 (red). The vertical component seismograms are bandpass filtered between 2.0 and 10.0 Hz. The station names, cross-correlation coefficients (γ) and differential traveltimes (T) are labelled above each waveform.

Table S1. Pn differential traveltimes at individual stations.

Table S2. Cross-correlation parameters of the Pn waveforms at individual stations.

Table S3. Event parameters used in this study.

(http://gji.oxfordjournals.org/lookup/suppl/doi:10.1093/gji/ggw239/-/DC1)

Please note: Oxford University Press is not responsible for the content or functionality of any supporting materials supplied by the authors. Any queries (other than missing material) should be directed to the corresponding author for the paper.